

Thermodynamics and Kinetics of Intramolecular Proton Transfer in Guanine. Post Hartree–Fock Study

Leonid Gorb,[†] Anna Kaczmarek,^{‡,§} Anastasiya Gorb,[§] Andrzej J. Sadlej,[‡] and Jerzy Leszczynski^{*,†}

Computational Center for Molecular Structure and Interactions, Department of Chemistry, Jackson State University, Jackson, Mississippi 39217, Department of Quantum Chemistry, Institute of Chemistry, Nicolaus Copernicus University, 7 Gagarin St., 87-100 Torun, Poland, and Dragomanov Pedagogical State University, 9 Pirogov Street, 01601 Kiev-30, Ukraine

Received: January 22, 2005; In Final Form: May 19, 2005

The most stable tautomers and rotamers of guanine are characterized by post Hartree–Fock ab initio calculations at the MP2 and CCSD(T) levels employing extended basis sets. Four of the lowest-energy structures (7*H*-oxo-amino- < 9*H*-oxo-amino- < 9*H*-syn-hydroxo-amino- < 9*H*-anti-hydroxo-amino-guanine) are found to lie within ca. 1 kcal/mol. The next form of guanine is established to lie more than 3 kcal/mol higher than the global minimum tautomer. The transition states of the following reversible reactions: 9*H*-oxo-amino-guanine \rightleftharpoons 9*H*-syn-hydroxo-amino-guanine \rightleftharpoons 9*H*-anti-hydroxo-amino-guanine have been studied. The calculated energy data were used to obtain thermodynamic parameters and to estimate the composition of the equilibrium mixture of conformers at 0 K and room temperature. The rate constants for the tautomerization of 9*H*-oxo-amino-guanine were determined by using the instanton approach. Their predicted values characterize an extremely slow chemical process, which is expected to reach the equilibrium in ca. 2500 h. Despite being so slow, we have shown that such a rate of the tautomerization describes a process that is much faster than the one characterized by the observed frequency of spontaneous point mutations. Therefore, additional stabilization factors, e.g., hydrations and interactions with enzymes are necessary to secure the known fidelity of DNA synthesis.

1. Introduction

Over the past years, computational investigations of molecules of biological interest have become an important tool that provide information about their structure and activity. Although the structure, tautomerism, and spectroscopic properties of nucleic acid bases have been extensively analyzed by experimentalists and computational chemists, one still finds several inconsistencies among different results. The interpretation of the experimental data is not unambiguous either.^{1–3} On the computational side,^{4–8} distinct conclusions seem to mainly arise from the uncertainty of different approximations, and DNA bases still remain a challenge for ab initio calculations at high levels of theory. The bottleneck in accurate quantum chemical calculations is the size of these molecules. The development of more efficient computational methods and the increase of computing power offer the possibility of improving upon earlier results. The reliability of the computed data for DNA bases becomes particularly important in the context of their possible tautomerization.

The continuous interest in structural and electronic features of DNA bases originates from attempts to explain the mechanism of spontaneous mutations in DNA in terms of the so-called “rare” tautomeric forms of these molecules. According to Watson and Crick, the canonical form of guanine (G) pairs with cytosine (C) by three hydrogen bonds.⁹ The “rare” guanine

tautomers mispair by creating the hydrogen bonds to thymine (T). Then, after the disconnection of the resulting DNA strands, thymine creates hydrogen bonds with adenine (A), and in the new DNA helix, one obtains the TA pair instead of CG.

DNA bases exhibit tautomerism that can be described by two types of structural changes. One of them is caused by the proton transfer from the heterocyclic ring nitrogen to the oxo- or imino-groups with the formation of –OH and –NH₂, respectively (keto–enol or imino–amino tautomerism). The second one, which occurs in purines, is a consequence of the mobility of the proton connected to the nitrogen in the imidazole ring. An example of these two tautomerization processes in guanine is shown in Scheme 1. It is worthwhile to note that the first of the exemplified tautomerization processes (see the first equation of the Scheme) will change the sense of complementarity. As for the second type of tautomerization (see the second equation of the Scheme), it is generally accepted that it does not have biological consequences because the 9H–9N bond of purines is substituted by a 9N–1'C bond in nucleosides and nucleotides.

The experimental data suggest that, up to the limit of sensibility of modern physical and chemical experimental methods, all DNA bases in polar solvents and in the condensed phase (crystals) exist exclusively in canonic form. In contrast, the presence of a number of cytosine and guanine tautomers unambiguously follows from the data of argon- and nitrogen-matrix and gas-phase experiments.^{1,2,10} However, the amount of these tautomers and the assignment of IR and UV transitions is still disputable.¹⁰

Because our paper is devoted to ab initio study of gas-phase distribution of guanine tautomers, it is worthwhile to discuss

* Corresponding author. E-mail: jerzy@ccmsi.us.

[†] Jackson State University.

[‡] Nicolaus Copernicus University.

[§] Dragomanov Pedagogical State University.

The figure illustrates the chemical structures and tautomeric transitions of four guanine derivatives. The top row shows the 9H-oxo-amino-guanine structure with atom numbering (1-9) and its equilibrium with the 9H-syn-hydroxo-amino-guanine structure via forward and reverse reactions. The 9H-syn-hydroxo-amino-guanine structure is in equilibrium with the 9H-anti-hydroxo-amino-guanine structure via forward and reverse reactions. The bottom row shows the equilibrium between the 9H-oxo-amino-guanine structure and the 7H-oxo-amino-guanine structure.

9H-oxo-amino-guanine

9H-syn-hydroxo-amino-guanine

9H-anti-hydroxo-amino-guanine

7H-oxo-amino-guanine

The geometry optimization and calculations of relative energies of the most stable conformers were performed with three Gaussian basis sets of increasing size and flexibility: 6-31G(d,p),¹⁵ 6-311++G(d,p),¹⁵ and aug-cc-pvdz.¹⁶ All geometries of the local minima and the transition state structures were

optimized without symmetry constraints by using these basis sets. The optimized Cartesian coordinates of all considered species are given in Supporting Information. The nature of all the stationary points determined from geometry optimizations has been established on the basis of the harmonic frequency data from MP2/6-311++G(d,p) calculations.

The conclusions obtained from the MP2 results were additionally verified by single-point calculations at the level of the coupled-cluster method with single and double excitations and with the perturbative estimation of the contribution attributable to three-body clusters at the CCSD(T)/aug-cc-pvdz//MP2/aug-cc-pvdz level of theory.

In most of computational studies of molecular structures and energies, the results are known to depend considerably on the choice of the basis set. This dependence can be investigated by using systematic sequences of basis sets and the extrapolation formulas for the so-called complete basis set limit (CBS). In the present case, these investigations have been carried out at the level of the MP2 approximation and for molecular geometries obtained in MP2/aug-cc-pVDZ calculations. The extrapolation of energies to the CBS limit was performed by using cc-pVXZ and aug-cc-pVXZ basis sets, where X stands for the basis set cardinal number $X = 2, 3, 4$.¹⁹

The use of different extrapolation schemes has been widely discussed by several authors. According to their conclusions,^{17–23} our study includes the extrapolation of the single-point MP2/cc-pVXZ and MP2/aug-cc-pVXZ energies as functions of the cardinal number X of the basis set by using the exponential formula,^{23,24}

$$E = E_{\infty} + A \exp(-BX) \quad (1)$$

and several inverse power formulas,^{23,24}

$$E = E_{\infty} + A/X^3 \quad (2)$$

$$E = E_{\infty} + A/X^3 + B/X^4 \quad (3)$$

$$E = E_{\infty} + A/X^4 + B/X^5 \quad (4)$$

$$E = E_{\infty} + A/X^3 + B/X^5 \quad (5)$$

where E is the energy obtained in single-point MP2 calculations for the given X , E_{∞} stands for the complete basis set limit energy, and A and B denote fitted parameters. All but the exponential fit were carried out analytically. In the case of the exponential form (1) the nonlinear least-squares Marquardt–Levenberg algorithm²⁴ as implemented in Gnuplot program was used.²⁵

We did not attempt to establish which of the extrapolation methods gives the most reliable CBS limits. Only a little is known about differences between CBS extrapolation schemes for large molecules of the size of guanine. Most of the validation of these formulas comes from the study of small systems and shows only a little distinction between most of them.^{17–24} Hence, only the plain CBS limits for relative energies will be presented.

The values of the Gibbs free energy changes, ΔG , and the equilibrium constants, K , have been calculated according to standard formulas, $\Delta G = \Delta H - T\Delta S$ and $K = \exp(-\Delta G/RT)$, at room temperature of 298.15 K. The calculated equilibrium constants were used to estimate the composition of the tautomer mixtures.²⁶

Because the tautomerization proceeding via proton transfer may involve the tunneling effect, the standard transition-state theory is not sufficient for the proper description of its dynamics. Multidimensional treatment of tunneling²⁷ is found to be

computationally very demanding. Thus, the instanton approach has been chosen in this study for the analysis of the tunneling process.^{28–31} This approach is based on the recognition that the tunneling amplitude depends exponentially on the barrier height separating the two tautomers. For the temperatures that are low in comparison to the barrier height, the effective tunneling trajectories are confined to a narrow region in the configuration space. This observation allows assumption of the one-dimensional characteristics for tunneling (the instanton path concept).^{28–31} The rate constant calculations require the inclusion of the adjacent trajectories, whose efficiency decreases with their distance from the instanton path.

The instanton approach as implemented in DOIT 1.2 code (Dynamics Of Instanton Tunneling) has been used to calculate rate constants for tautomerization processes in guanine.^{28–31} The energy barrier and the exothermicity of the proton transfer have been computed at the MP2/6-311++G(d,p) level of the theory.

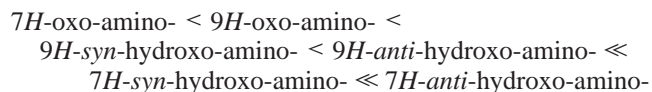
To describe the kinetics of the tautomeric transitions in guanine molecule that are presented in the first line of Scheme 1, we have considered a two-step first-order reversible reaction^{32,33} of the tautomerization from the *oxo* (A) to *anti-hydroxo* (C) product which goes through the *syn-hydroxo* (B) conformer



where k_1^f , k_1^r , k_2^f , and k_2^r denote the rate constants for the forward and the reverse reaction, respectively. The system of differential equations and its analytical solution are presented in Supporting Information.

3. Results and Discussion

3.1. Low-Energy Tautomers of Guanine: Relative Energies. The relative energies of four guanine tautomers and two rotamers are given in Table 1. The 7*H*-oxo-amino- tautomer always has the lowest energy. At the MP2 level, the order of relative energies is always the same:



One finds that the four lowest-energy species all lie within the energy range of less than 2 kcal/mol. This feature is method independent. However, the relative ordering of the three higher-energy tautomers depends on the method.

The comparison of these data with the results using different techniques, which extrapolate the results to the complete basis set, slightly changed the picture. 7*H*-oxo-amino-tautomer continues to possess the lowest energy. However, on the first glance, the order of relative energies is not the constant and depends on the extrapolation methods used. A more careful look at the data presented in Table 1 enable us to make a different conclusion. First of all, we would like to highlight that all extrapolation methods suggest a significantly lower energy gap between the lowest tautomer and the last one. This energy gap is predicted in the range of 0.49–1.17 kcal/mol. Such a small energy difference approaches the accuracy of applied quantum chemical methods.

3.2. Low-Energy Tautomers of Guanine: Thermodynamics. A very small difference in relative energies of guanine tautomers suggests that, in a gas phase, the molecule should actually exist as the mixture of tautomers. However, the difference in relative energies corresponds just to the relative

TABLE 1: Relative Energies (in kcal/mol) of Selected Low-Energy Conformers of Guanine

	MP2/ 6-31G(d,p)	MP2/ 6-311++G(d,p)	MP2/ aug-cc-pvdz	$E_{\text{MP2}} =$ $E_{\infty} +$ $A \exp(-BX)$ $X = 2, 3, 4$	$E_{\text{MP2}} =$ $E_{\infty} + A/X^3$ $+ B/X^4$ $X = 2, 3, 4$	$E_{\text{MP2}} =$ $E_{\infty} + A/X^4$ $+ B/X^5$ $X = 2, 3, 4$	$E_{\text{MP2}} =$ $E_{\infty} + A/X^3$ $+ B/X^5$ $X = 2, 3, 4$	$E_{\text{MP2}} =$ $E_{\infty} + A/X^3$ $X = 2, 3$	CCSD(T)/ aug-cc-pvdz// MP2/ aug-cc-pvdz
7H-oxo-amino-	0.0	0.0	0.0	0.0	0.0	0.0	0.0	0.0	0.0 (0.0) ^a
9H-oxo-amino-	0.06	0.29	0.72	0.70	0.70	0.72	0.68	0.73	0.77 (0.48) ^a
9H-syn-hydroxo-amino-	1.13	0.80	1.06	1.05	0.46	0.90	0.28	0.74	1.64 (0.49) ^a
9H-anti-hydroxo-amino-	1.79	1.00	1.30	1.17	0.64	1.02	0.49	0.85	1.27 (0.82) ^a
7H-syn-hydroxo-amino-	4.46	3.59	3.5	3.87	3.34	3.70	3.20	3.57	3.69 (3.01) ^a
7H-anti-hydroxo-amino-	13.15	11.65	11.1						

^a The data are taken from ref 10d and recalculated using relative Gibbs free energy of 7H-oxo-amino-guanine as reference point.

TABLE 2: Relative Enthalpies (in kcal/mol) and Composition of Equilibrium Mixture at 0 K (in percent) of Selected Low-Energy Conformers of Guanine

	MP2/ 6-31G(d,p)	MP2/ 6-311++G(d,p)	MP2/ aug-cc-pvdz	$E_{\text{MP2}} =$ $E_{\infty} +$ $A \exp(-BX)$ $X = 2, 3, 4$	$E_{\text{MP2}} =$ $E_{\infty} + A/X^3$ $+ B/X^4$ $X = 2, 3, 4$	$E_{\text{MP2}} =$ $E_{\infty} + A/X^4$ $+ B/X^5$ $X = 2, 3, 4$	$E_{\text{MP2}} =$ $E_{\infty} + A/X^3$ $+ B/X^5$ $X = 2, 3, 4$	$E_{\text{MP2}} =$ $E_{\infty} + A/X^3$ $X = 2, 3$	CCSD(T)/ aug-cc-pvdz// MP2/ aug-cc-pvdz
7H-oxo-amino-	0.0,	0.0,	0.0,	0.0,	0.0,	0.0,	0.0,	0.0,	0.0 (0.0), ^a
	15.8	28.2	91.00	88.51	33.49	13.7	85.40	71.59	94.9 (89.88)
9H-oxo-amino-	-0.25,	-0.03,	0.41,	0.36,	0.38,	0.36,	0.41,	0.41,	0.45 (0.44), ^a
	83.8	34.45	5.92	8.04	2.66	1.24	5.55	4.65	4.73 (4.79)
9H-syn-hydroxo-amino-	0.59,	-0.04,	0.52,	0.51,	-0.08,	-0.26,	0.36,	0.19,	1.10 (0.45), ^a
	0.31	36.82	2.84	2.96	57.08	77.52	7.75	20.18	0.06 (4.50)
9H-anti-hydroxo-amino-	1.39,	0.60,	0.90,	0.78,	0.24,	0.09,	0.63,	0.45,	0.87 (0.70), ^a
	0.00	0.51	0.22	0.49	6.76	7.52	1.28	3.56	0.28 (0.85)
7H-syn-hydroxo-amino-	4.2,	3.15,	3.40,	3.42,	2.90,	3.26,	2.76,	3.13,	3.25 (3.17), ^a
	0.00	0.00	0.00	0.00	0.00	0.00	0.00	0.00	0.00 (0.00)

^a The data are taken from ref 10d and recalculated using relative Gibbs free energy of 7H-oxo-amino-guanine as reference point.

TABLE 3: Relative Gibbs Free Energies (in kcal/mol) and Composition of Equilibrium Mixture at 298.15 K (in percent) of Selected Low-Energy Conformers of Guanine

	MP2/ 6-31G(d,p)	MP2/ 6-311++G(d,p)	MP2/ aug-cc-pvdz	$E_{\text{MP2}} =$ $E_{\infty} +$ $A \exp(-BX)$ $X = 2, 3, 4$	$E_{\text{MP2}} =$ $E_{\infty} + A/X^3$ $+ B/X^4$ $X = 2, 3, 4$	$E_{\text{MP2}} =$ $E_{\infty} + A/X^4$ $+ B/X^5$ $X = 2, 3, 4$	$E_{\text{MP2}} =$ $E_{\infty} + A/X^3$ $+ B/X^5$ $X = 2, 3, 4$	$E_{\text{MP2}} =$ $E_{\infty} + A/X^3$ $X = 2, 3$	CCSD(T)/ aug-cc-pvdz// MP2/ aug-cc-pvdz
7H-oxo-amino-	0.0,	0.0,	0.0,	0.0,	0.0,	0.0,	0.0,	0.0,	0.0 (0.0), ^a
	8.30	17.79	83.96	79.9	23.5	8.82	76.62	60.46	90.82 (92.57)
9H-oxo-amino-	-0.36,	-0.13,	0.30,	0.25,	0.28,	0.26,	0.30,	0.31,	0.35 (0.44), ^a
	91.42	42.31	11.37	15.1	3.64	1.56	10.37	7.66	8.81 (4.93)
9H-syn-hydroxo-amino-	0.51,	-0.12,	0.44,	0.43,	-0.16,	-0.34,	0.28,	0.11,	1.02 (0.56), ^a
	0.27	39.57	4.47	4.55	68.37	85.01	11.85	29.05	0.10 (2.22)
9H-anti-hydroxo-amino-	1.39,	0.60,	0.91,	0.78,	0.25,	0.1,	0.63,	0.46,	0.88 (0.87), ^a
	0.00	0.32	0.20	0.44	4.44	4.53	1.15	2.82	0.25 (28)
9H-anti-hydroxo-amino-	4.04,	3.17,	3.43,	3.45,	2.92,	3.38,	2.78,	3.15,	3.27 (3.29), ^a
	0.00	0.00	0.00	0.00	0.00	0.00	0.00	0.00	0.00 (0.00)

^a The data are taken from ref 10d and recalculated using relative Gibbs free energy of 7H-oxo-amino-guanine as reference point.

order of the minima on the potential energy surface. To predict the order of relative stability, one should include zero-point (thermal) and entropy corrections. To investigate the influence of these parameters, we have calculated the order of relative stability and the distribution of the tautomers at the thermodynamic equilibrium at 0 and 298.15 K. The results are collected in the Table 2 and Table 3.

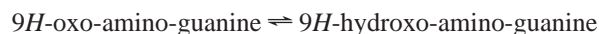
Because the energy difference between the tautomers is small, one should not be surprised that the zero-point energy, thermal corrections, entropy, and the temperature significantly affect the predicted composition of the thermodynamically equilibrated mixture. In particular, a relatively small difference of ca. 0.1 kcal/mol between corresponding values of the relative enthalpy and relative Gibbs free energy results in significant change of the composition of the equilibrium mixture.

All calculations presented in this paper consistently predict that the equilibrium mixture should be dominated by four tautomers that correspond to the lowest-energy forms of guanine found in this study. However, only three of them are those of the four tautomers observed experimentally. According to our data, the equilibrium concentration of 7H-syn-hydroxo-amino-guanine, which possibly was observed in experiments of Mons et al.,¹⁰ should be negligible. There seems to be hardly a chance that improving upon the basis sets and computational methods would lead to large enough lowering of its relative energy and make its equilibrium concentration observable. Hence, one can conclude that, most likely, the tautomeric mixture observed experimentally is not equilibrated either at 0 K or at room temperature. In other words the experimental conditions might not correspond to the thermodynamic equilibrium, and the results

of calculations should not be compared to the experimentally determined relative concentration of different guanine tautomers.

Most of the computed data, including those recently published by Hanus et al.,^{10d} suggest that the 7*H*-oxo-amino- tautomer should be the dominant form of guanine. Only in two cases, which correspond to MP2/6-31G(d,p) and MP2/6-311++G(d,p) data, the 9*H*-oxo-amino form is dominant. It is also interesting to note that results of MP2/6-311++G(d,p), MP2/aug-cc-pvdz calculations and the present CBS estimates predict almost the same fraction of the 9*H*-oxo-amino- and 9*H*-syn-hydroxo-amino- tautomers as that found by Hanus et al.^{10d}

3.3. Low-Energy Tautomers of Guanine: Kinetics of Intramolecular Proton Transfer. Simple kinetic models of the guanine tautomerization on the basis of its two forms only have been considered in our recent papers.³⁴ They were based on the computed rate constants and the solution of the kinetic equation, which corresponds to a single reversible reaction and the scheme.



The present study considers a more realistic kinetic model, which is represented in Scheme 1 and eq 6. This model is meant to correspond to biologically relevant pathway of proton transfer between different forms of guanine, and for this reason, unlikely 7*H*–9*H* tautomerism (see Table 3) is neglected in our considerations. No extrapolation to the complete basis set limit has been carried out for the barrier height to intramolecular proton transfer. In contrast to the relative stabilities, the heights of the barriers have been found to be very sensitive to the level of approximation and do not seem to permit a justified extrapolation.³⁵

With the 7*H*-oxo-amino- tautomer excluded from further considerations, the composition of the thermodynamically equilibrated mixture will be reduced to one of the following two possibilities. According to the results of the MP2/6-31G(d,p) and CCSDT/aug/cm³-pvdz//MP2/aug-cc-pvdz approximations, the mixture will be dominated by the 9*H*-oxo-amino-guanine form (more than 90%). Alternatively, as suggested by the MP2/6-311++G(d,p) and MP2/aug-cc-pvdz levels data and by the results published in ref 10c, the mixture should contain approximately equal concentrations of 9*H*-oxo-amino- and 9*H*-syn-hydroxo-amino- forms. To be more specific, let us focus on the MP2/6-311++G(d,p) data. Because the 9*H*-oxo-amino-guanine is dominant in both crystals and living cells, the acceptable kinetics of proton transfer may anticipate the 9*H*-oxo-amino-form as the reagent and different hydroxo-forms as products. Following these considerations, the results of MP2/6-311++G(d,p) calculations predict at 298.18 K the ratio of 9*H*-oxo-amino-/9*H*-syn-hydroxo-amino-/9*H*-anti-hydroxo-amino- forms as given by 51.5:48.1:0.4.

The ab initio predicted kinetic parameters of the investigated tautomerization processes are presented in Table 4. It is rather surprising to find that the barrier value for proton transfer between 9*H*-oxo-amino- and 9*H*-hydroxo-amino-guanine forms is significantly higher than the barrier of syn/anti hydroxyl group rotation. This results in relative values of rate constants, which, as compared to syn/anti hydroxyl rotation, are approximately 10 orders smaller for the tautomerization of 9*H*-oxo-amino- to the 9*H*-hydroxo-amino- form. This conclusion holds for both zero and room temperatures. Moreover, one notes that the value of the rate constant for the 9*H*-oxo-amino to 9*H*-syn-hydroxo-amino transition reflects an extremely small rate of proton transfer.

The plot of the kinetic data predicted by our calculations (DOIT 1.2 program) is presented in Figure 1. These data

TABLE 4: Kinetic Parameters of 9*H*-oxo-amino- \rightleftharpoons 9*H*-syn-hydroxo-amino- \rightleftharpoons 9*H*-anti-hydroxo-amino- Transitions Calculated at MP2/6-311++G(d,p) Level

	9 <i>H</i> -oxo-amino- \rightleftharpoons 9 <i>H</i> -syn-hydroxo-	9 <i>H</i> -syn-hydroxo-amino- \rightleftharpoons 9 <i>H</i> -anti-hydroxo-amino-
ΔE^\ddagger (kcal/mol)	37.28	8.78
ΔH_0^\ddagger (kcal/mol)	33.88	7.98
ΔG_{298}^\ddagger (kcal/mol)	33.72	8.09
k_0^f (s ⁻¹) ^a	1.05×10^{-13}	17.3
k_0^r (s ⁻¹) ^b	0.98×10^{-13}	1.27×10^3
k_{298}^f (s ⁻¹) ^a	2.2×10^{-7}	6.9×10^6
k_{298}^r (s ⁻¹) ^b	2.35×10^{-7}	1.8×10^8

^a k_0^f , k_{298}^f denote the rate constants for the forward reaction of tautomerization in the temperature 0 K and 298 K, respectively. ^b k_0^r , k_{298}^r denote the rate constants for the reverse reaction of tautomerization in the temperature 0 K and 298 K, respectively.

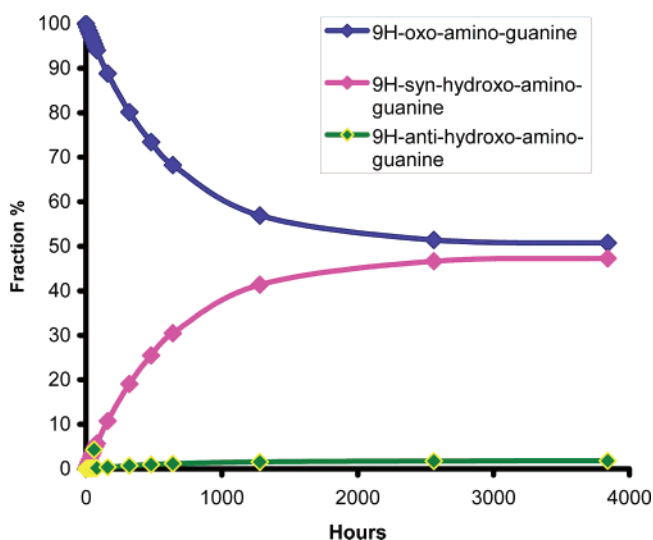


Figure 1. Ab initio predicted kinetics of intramolecular proton transfer in 9*H*-oxo-amino-guanine.

correspond to Scheme 1 and eq 6 at room temperature. The gas-phase tautomerization processes turn out to be a very slow chemical reaction that approaches the equilibrium concentration in about 2500 h (104 days). According to these data, we concluded that the significant amount of different guanine tautomers observed in gas-phase and matrix experiments should follow from some alternative pathways such as tautomerization via the UV excitation in the case of IR–UV depletion studies.¹⁰ These experiments start from the guanine crystal, in which no observable concentration of hydroxo-amino-guanine form is present.

We also modeled similar kinetics at 0 K. We did not plot it on the graph because our results predict virtually no transformation of guanine even in 2500 h.

Despite the predicted low rate for 9*H*-oxo-amino- and 9*H*-syn-hydroxo-amino-guanine transformation, our results suggest the possible importance of such chemical transformation in the pathway of DNA spontaneous point mutations. Indeed, the frequencies of spontaneous GC \rightarrow AT transitions in *E. coli* is determined to be on the order of 10^{-10} per nucleotide synthesized.³⁶ This means that the relative concentration of guanine hydroxo-amino forms that is greater than ca. 10^{-10} needs to be in some way diminished, e.g., by hydration, interactions with enzymes (DNA polymerase), etc. To illustrate this point, let us consider the kinetics of proton transfer during the first 1000 s. This time is chosen as close to the period required to generate a cell of *E. coli*³⁷ and is of the same order of magnitude as the

TABLE 5: Kinetics of 9H-syn-hydroxo-amino and 9H-anti-hydroxo-amino-guanine Appearance during the First 1000 s of the Tautomerization Process

time (s)	fraction (%)	
	9H-syn-hydroxo-amino-guanine	9H-anti-hydroxo-amino-guanine
0	0	0
0.01	2.12E-09	8.12E-11
0.1	2.12E-08	8.12E-10
1	2.12E-07	8.12E-09
10	2.12E-06	8.12E-08
100	2.12E-05	8.12E-07
1000	2.12E-04	8.12E-06

time of DNA synthesis in this cell. The data presented in Table 5 show that, after 0.1 s, the relative concentrations of the hydroxo- forms significantly exceed the natural frequency of spontaneous GC \rightarrow AT transitions. Hence, the reaction, which is very slow from chemical point of view, is still too fast to ensure naturally observed fidelity of DNA synthesis. This conclusion agrees with the well-established views that spontaneous chemical reactions are too fast to yield the observed rate of spontaneous mutation.^{37,38} In the living cell, errors introduced during the synthesis of DNA can be further decreased by hydration and corrected by a “proofreading” mechanism sustained by DNA polymerases. However, the influence of the mentioned factors should also be investigated with care because, for example, recent data suggest that the hydration by a selected number of water molecules can either stabilize or destabilize canonical forms of guanine, depending on the position of the attachment of water.³⁹

Finally, we would like to analyze briefly the chemical and biological consequences that follow from the data predicting the predominance of the 9H-oxo-amino-guanine form. This particular case can be considered in terms of the MP2/6-31G(d,p) and CCSD(T)-aug-cc-pvdz//MP2/aug-cc-pvdz results. The former data are of low quality concerning both the basis set and the level of approximation. Therefore, we shall consider only CCSD(T)/aug-cc-pvdz//MP2/aug-cc-pvdz results and use the rate constants obtained at the MP2/6-311++G(d,p) level.

According to the CCSD(T)/aug-cc-pvdz//MP2/aug-cc-pvdz data, the ratio of 9H-oxo-amino/9H-syn-hydroxo-amino/9H-anti-hydroxo-amino- forms is 96.1:1.1:2.8. Hence, in this case, the time to reach equilibrium should be quite short. Its present estimate amounts to about 50 h. Because this time still is much longer than 1000 s \approx 0.3 h, we conclude that the biological implications do not depend on the level of theory applied in the study.

4. Summary and Conclusions

We have investigated several low-energy tautomers of guanine and intramolecular proton transfer between its 9H-oxo-amino- and 9H-hydroxo-amino-forms by using different basis sets and high-level-correlated methods of the electronic structure theory. Our calculations show that there are four tautomers of guanine that have the relative energies in the range of approximately 1 kcal/mole. They also confirm the earlier findings that, in the gas phase, the 7H-oxo-amino structure represents the lowest-energy tautomer. The new most important conclusions are the follows:

1. The analysis of the computed data suggests that there should be at most four tautomers of guanine present in the mixture at both 0 K and room temperatures. However, one of them is not yet observed experimentally.

2. The theoretically predicted values of the rate constants suggest that 9H-oxo-amino-9H-hydroxo-amino- intramolecular

proton transfer in guanine proceeds as an extremely slow chemical reaction. The equilibrium concentration of tautomers might be eventually reached at approximately 2500 h. Taking into account that only three of four low-energy tautomers are observed experimentally, we concluded that the most likely tautomeric mixture observed experimentally is not equilibrated either at 0 K or at room temperature.

3. With respect to the kinetics of 9H-oxo-amino-9H-hydroxo-amino- tautomerization, we have shown that such a slow chemical reaction still could be considered as the source of point mutations. However, stabilization factors, such as hydration and the interactions with enzymes, are necessary to change the thermodynamics and/or kinetics of this reaction into the range that correlates with the experimentally observed fidelity of DNA replication.

Acknowledgment. This work was facilitated by the support of NSF CREST grant No. HRD-0318519, HIH-SCORE grant No. SO6 GMO08047 and by support of the Army High Performance Computing Research Center under the auspices of the Department of the Army, Army Research Laboratory cooperative agreement number DAAHO4-95-2-0003, contract number DAAHO4-95-C-0008, the content of which does not necessarily reflect the position or the policy of the government, and no official endorsement should be inferred. The authors wish to thank the Mississippi Center for Supercomputing for the use of computational facilities. The authors would like to acknowledge valuable suggestions and comments of reviewers.

Supporting Information Available: System of differential kinetic equations that corresponds to eq 6 and analytical solution for it; Cartesian coordinates of all considered in the paper species, optimized at the MP2/6-31G(d,p), MP2/6-311++G(d,p), and MP2/aug-cc-pvdz levels of theory. This material is available free of charge via the Internet at <http://pubs.acs.org>.

References and Notes

- (1) (a) Piuze, F.; Mons, M.; Dimicoli, I.; Tardivel, B.; Zhao, Q. *Chem. Phys.* **2001**, 270, 205. (b) Szczepaniak, K.; Szczepaniak, M.; *J. Mol. Struct.* **1987**, 156, 29. (c) Sheina, G. G.; Stepanian, E. D.; Radchenko, E. D.; Blagoi, Yu. P. *J. Mol. Struct.* **1987**, 158, 275.
- (2) (a) Nir, E.; Janzen, C.; Imhof, P.; Kleinermanns, K.; de Vries, M. S. *J. Chem. Phys.* **2001**, 115, 4604. (b) Nir, E.; Grace, L.; Brauer, B.; de Vries, M. S. *J. Am. Chem. Soc.* **1999**, 121, 4896.
- (3) Nir, E.; Kleinermanns, K.; Grace, de Vries, M. S. *J. Phys. Chem. A* **2001**, 105, 5106.
- (4) Kwiatkowski, S. J.; Leszczynski, J. *J. Mol. Struct. (THEOCHEM)* **1990**, 208, 35.
- (5) Tian, S. X.; Xu, K. Z. *Chem. Phys.* **2001**, 264, 187.
- (6) Leszczynski, J. *J. Phys. Chem. A* **1998**, 102, 2357.
- (7) Leszczynski, J. *Chem. Phys. Lett.* **1990**, 174, 347.
- (8) Gould, I. R.; Hillier, I. H. *Chem. Phys. Lett.* **1989**, 161, 185.
- (9) Watson, J. D.; Crick, F. H. *Nature* **1953**, 171, 4356.
- (10) (a) Mons, M.; Dimicoli, I.; Piuze, F.; Tardivel, B.; Elhanine, J. *Phys. Chem. A* **2002**, 106, 5088. (b) Chin, W.; Mons, M.; Dimicoli, I.; Piuze, F.; Tardivel, B.; Elhanine, M. *Eur. Phys. J. D* **2002**, 20, 347. (c) Chin, W.; Mons, M.; Piuze, F.; Tardivel, B.; Dimicoli, I.; Gorb, L.; Leszczynski, J. *J. Phys. Chem. A* **2004**, 108, 8237. (d) Hanus, M.; Ryjacek, F.; Kabelac, M.; Kubart, T.; Bogdan, T. V.; Trygubenko, S. A.; Hobza, P. *J. Am. Chem. Soc.* **2003**, 125, 7678.
- (11) Colominas, C.; Luque, F.; Orozco, M. *J. Am. Chem. Soc.* **1996**, 118, 6811.
- (12) Sabio, M.; Topiol, S.; Lumma, W. C., Jr. *J. Phys. Chem.* **1990**, 94, 1366.
- (13) Leao, M. B. C.; Longo, R. L.; Pavao, A. C. *J. Mol. Struct. (THEOCHEM)* **1999**, 145.
- (14) Frisch, M. J.; Trucks, G. W.; Schlegel, H. B.; Scuseria, G. E.; Robb, M. A.; Cheeseman, J. R.; Zakrzewski, V. G.; Montgomery, J. A., Jr.; Stratmann, R. E.; Burant, J. C.; Dapprich, S.; Millam, J. M.; Daniels, A. D.; Kudin, K. N.; Strain, M. C.; Farkas, O.; Tomasi, J.; Barone, V.; Cossi,

- M.; Cammi, R.; Mennucci, B.; Pomelli, C.; Adamo, C.; Clifford, S.; Ochterski, J.; Petersson, G. A.; Ayala, P. Y.; Cui, Q.; Morokuma, K.; Malick, D. K.; Rabuck, A. D.; Raghavachari, K.; Foresman, J. B.; Cioslowski, J.; Ortiz, J. V.; Stefanov, B. B.; Liu, G.; Liashenko, A.; Piskorz, P.; Komaromi, I.; Gomperts, R.; Martin, R. L.; Fox, D. J.; Keith, T.; Al-Laham, M. A.; Peng, C. Y.; Nanayakkara, A.; Gonzalez, C.; Challacombe, M.; Gill, P. M. W.; Johnson, B. G.; Chen, W.; Wong, M. W.; Andres, J. L.; Head-Gordon, M.; Replogle, E. S.; Pople, J. A. *Gaussian 98*, revision A.9; Gaussian, Inc.: Pittsburgh, PA, 1998.
- (15) Hehre, W. J.; Radom, L.; Schleyer, P. v. R.; Pople, J. A. *Ab Initio Molecular Orbital Theory*, John Wiley & Sons: New York, 1986.
- (16) Dunning, T. H. *J. Chem. Phys.* **1989**, *90*, 1007.
- (17) Lee, J. S.; Park, S. Y. *J. Chem. Phys.* **2000**, *112*, 10746.
- (18) Varandas, A. J. C. *J. Chem. Phys.* **2000**, *113*, 8880.
- (19) Truhlar, D. G. *Chem. Phys. Lett.* **1998**, *294*, 45.
- (20) Helkager, T.; Klopper, W.; Koch, H.; Noga, J. *J. Chem. Phys.* **1997**, *106*, 9639.
- (21) Martin, J. M. L. *Chem. Phys. Lett.* **1996**, *259*, 669.
- (22) Feller, D. *J. Chem. Phys.* **1992**, *96*, 6104.
- (23) Feller, D. *J. Chem. Phys.* **1993**, *98*, 7059.
- (24) Marquardt, D. W. *J. Soc. Ind. Appl. Math.* **1963**, *11*, 431.
- (25) Williams, T.; Kelley, C.; GNUPLOT An Interactive Plotting Program, version 3.7.
- (26) Ochterski, J. W. www.gaussian.com/thermo.htm, Thermochemistry in Gaussian.
- (27) (a) Truhlar, D. G.; Garret, B. C. *Acc. Chem. Res.* **1980**, *13*, 440. (b) Truhlar, D. G.; Issacson, A. D.; Garret, B. C. In *Theory of Chemical Reactions Dynamics*; Baer, M., Ed.; CRC: Boca Raton, FL, 1985; Vol. 4, pp 65–137. (c) Tucker, S. C.; Truhlar, D. G. In *New Theoretical Concepts for Understanding Organic Reactions*; Bertran, J., Csizmadia, I. G., Eds.; Kluwer: Dordrecht, The Netherlands, 1989; pp 291–346. (d) Hase, W. L. *Acc. Chem. Res.* **1983**, *16*, 258. (e) Keck, J. C. *Adv. Chem. Phys.* **1967**, *13*, 85.
- (28) Smedarchina, Z.; Siebrand, W.; Fernandez-Ramos, A.; Gorb, L.; Leszczynski, J. *J. Chem. Phys.* **2000**, 566.
- (29) Smedarchina, Z.; Fernandez-Ramos, A.; Siebrand, W. *J. Comput. Chem.* **2001**, 787.
- (30) Smedarchina, Z.; Fernandez-Ramos, A.; Zgierski, M. Z.; Siebrand, W. *DOIT 1.2*, A Computer Program to Calculate Hydrogen Tunneling Rate Constants and Splittings; National Research Council of Canada: Ottawa.
- (31) Smedarchina, Z.; Siebrand, W.; Fernandez-Ramos, A.; Zgierski, M. Z.; Zerbetto, F. *J. Chem. Phys.* **1995**, 7024.
- (32) Steinfeld, J. I.; Francisco, S. J.; Hase, W. L. *Chemical Kinetics and Dynamics*; Prentice Hall: Englewood Cliffs, New Jersey, 1989.
- (33) Starzak, M. E. *Mathematical Methods in Chemistry and Physics*. Plenum Press: New York, 1989.
- (34) (a) Podolyan, Y.; Gorb, L.; Leszczynski, J. *Int. J. Mol. Sci.* **2003**, *4*, 410. (b) Gorb, L.; Podolyan, Y.; Leszczynski, J.; Siebrand, W.; Fernandez-Ramos, A.; Smedarchina, Z. *Biopolym. (Nucleic Acid Sci.)* **2002**, *61*, 77.
- (35) Gorb, L.; Leszczynski, J. *J. Am. Chem. Soc.* **1998**, *120*, 5024.
- (36) Fowler, R. G.; Degnen, G. E.; Cox, E. C. *Mol. Gen. Genet.* **1974**, *133*, 179.
- (37) Stent, G. S.; Calendar, B. *Molecular Genetics: An Introductory Narrative*; W. H. Freeman: New York, 1978.
- (38) (a) Kornberg, A. *DNA Synthesis*; W. H. Freeman: San Francisco, 1974. 17. (b) Watson, J. D. *Molecular Biology of Genes*; W. A. Benjamin: New York, 1970.
- (39) Hu, Xingbang; Li, Haoran; Liang, Wanchun; Han, Shijun *J. Phys. Chem. B* **2004**, *108*, 12999.